Path integral Liouville dynamics for thermal equilibrium systems

Jian Liu

Citation: J. Chem. Phys. **140**, 224107 (2014); doi: 10.1063/1.4881518
View online: https://doi.org/10.1063/1.4881518
View Table of Contents: http://aip.scitation.org/toc/jcp/140/22
Published by the American Institute of Physics

Path integral Liouville dynamics for thermal equilibrium systems

Jian Liu[a)]
Beijing National Laboratory for Molecular Sciences, Institute of Theoretical and Computational Chemistry, College of Chemistry and Molecular Engineering, Peking University, Beijing 100871, China

(Received 20 March 2014; accepted 23 May 2014; published online 11 June 2014)

We show a new imaginary time path integral based method—path integral Liouville dynamics (PILD), which can be derived from the equilibrium Liouville dynamics [J. Liu and W. H. Miller, J. Chem. Phys. **134**, 104101 (2011)] in the Wigner phase space. Numerical tests of PILD with the simple (white noise) Langevin thermostat have been made for two strongly anharmonic model problems. Since implementation of PILD does not request any specific form of the potential energy surface, the results suggest that PILD offers a potentially useful approach for general condensed phase molecular systems to have the two important properties: conserves the quantum canonical distribution and recovers exact thermal correlation functions (of even nonlinear operators, i.e., nonlinear functions of position or momentum operators) in the classical, high temperature, and harmonic limits. © *2014 AIP Publishing LLC*. [http://dx.doi.org/10.1063/1.4881518]

I. INTRODUCTION

There is currently considerable effort focused on developing ways for including quantum mechanical effects in condensed phase molecular dynamics simulations.[1–5,19] Several classes of trajectory-based dynamics methods have been proposed for simulating quantum correlation functions for large molecular systems in thermal equilibrium, since most dynamical quantities of interest can be expressed in terms of time correlation functions[6–8] that are of the form

$$C_{AB}(t) \equiv \langle \hat{A}(0)\hat{B}(t)\rangle = \frac{1}{Z}\mathrm{Tr}(\hat{A}^{\beta} e^{i\hat{H}t/\hbar}\hat{B}e^{-i\hat{H}t/\hbar}), \qquad (1)$$

where $\hat{A}^{\beta} = e^{-\beta\hat{H}}\hat{A}$ for the standard version of the correlation function, or $\hat{A}^{\beta}_{Kubo} = \frac{1}{\beta}\int_0^{\beta} d\lambda\, e^{-(\beta-\lambda)\hat{H}}\hat{A}e^{-\lambda\hat{H}}$ for the Kubo-transformed version. Here, $Z = \mathrm{Tr}[e^{-\beta\hat{H}}]$ ($\beta = 1/k_B T$) is the partition function, $\hat{H}$ the (time-independent) Hamiltonian of the system with the total number of degrees of freedom N, which we assume to be of standard Cartesian form

$$\hat{H} = \frac{1}{2}\hat{\mathbf{p}}^{T}\mathbf{M}^{-1}\hat{\mathbf{p}} + V(\hat{\mathbf{x}}), \qquad (2)$$

where $\mathbf{M}$ is the diagonal "mass matrix," and $\hat{\mathbf{p}}$ and $\hat{\mathbf{x}}$ are the momentum and coordinate operators, respectively; and $\hat{A}$ and $\hat{B}$ are operators relevant to the specific property of interest. These trajectory-based methods include the linearized semiclassical initial value representation (LSC-IVR)/classical Wigner,[9–15] derivative forward-backward semiclassical dynamics (FBSD),[16–20] centroid molecular dynamics (CMD),[3,21–24] and ring polymer molecular dynamics (RPMD),[4,25–28] etc.

More recently, we have proposed three families of approaches in phase space formulations of quantum mechanics[29–32] [equilibrium Liouville dynamics (ELD), equilibrium continuity dynamics, and equilibrium Hamiltonian dynamics (EHD)] that are able to combine the important properties of LSC-IVR/FBSD and of CMD/RPMD. That is,

1. conserve the quantum canonical density distribution function for the thermal equilibrium system; and
2. treat both linear and *nonlinear* operators (i.e., linear and *nonlinear* functions of position or momentum operators) equally well and recover exact thermal correlation functions in the classical ($\hbar \to 0$), high temperature ($\beta \to 0$), and harmonic limits.

Several methodologies (such as the Feynman-Kleinert approximation and thermal Gaussian approximations in the position state or coherent state representation, etc.) have been presented for the applications of these three families of trajectory-based dynamics[29,31,32] for describing quantum dynamic effects for thermal equilibrium systems. These methodologies are efficient when the potential of the system can be represented by polynomials, exponential, or Gaussian functions. However, Gaussian averages in these methodologies become computational demanding for complex molecular systems where angle and dihedral interactions (or induced dipole-dipole interactions) are important and accurate polynomial, exponential, or Gaussian fitting of potential surfaces is often intractable. It would thus be appealing to develop a methodology that does not require any specific form of the potential energy surface and is then in principle feasible to be combined with *ab initio* calculations on the fly.

The purpose of this paper is to present a path integral representation of the ELD in the Wigner phase space and to test them with standard model problems. Section II first briefly summarizes the ELD approach and discusses the expression of the effective force in the Wigner phase space. Section III proposes a path integral representation based on the staging transformation for evaluating the effective force, then shows how a molecular dynamics scheme can be constructed by introducing an adiabatic parameter. Section IV presents another point of view to derive this methodology from EHD in the spirit of the Hamilton equations of motion. Some numerical tests are demonstrated in Sec. V, including a strongly anharmonic oscillator, and a more challenging quartic well. Concluding remarks are given in Sec. VI.

a)Electronic mail: jianliupku@pku.edu.cn

II. EQUILIBRIUM LIOUVILLE DYNAMICS

A. Theory

Following Refs. 29–31, one can express Liouville's theorem in quantum mechanics in the Wigner or Husimi phase space as

$$\frac{\partial \rho^{\rm eq}(\mathbf{x},\mathbf{p};{\rm t})}{\partial {\rm t}} = -\mathbf{p}^{\rm T}\mathbf{M}^{-1}\frac{\partial \rho^{\rm eq}}{\partial \mathbf{x}} + \left(\frac{\partial \rho^{\rm eq}}{\partial \mathbf{p}}\right)^{\rm T}\cdot\frac{\partial {\rm V}_{\rm eff}(\mathbf{x},\mathbf{p})}{\partial \mathbf{x}}. \tag{3}$$

The following equality always holds:

$$\frac{d\rho^{\rm eq}(\mathbf{x}_{\rm t},\mathbf{p}_{\rm t};t)}{dt} = \frac{\partial \rho^{\rm eq}(\mathbf{x}_{\rm t},\mathbf{p}_{\rm t};t)}{\partial t} + \frac{\partial \rho^{\rm eq}(\mathbf{x}_{\rm t},\mathbf{p}_{\rm t};t)}{\partial \mathbf{x}_{\rm t}}\cdot\dot{\mathbf{x}}_{\rm t} + \frac{\partial \rho^{\rm eq}(\mathbf{x}_{\rm t},\mathbf{p}_{\rm t};t)}{\partial \mathbf{p}_{\rm t}}\cdot\dot{\mathbf{p}}_{\rm t}. \tag{4}$$

If the trajectory in the phase space is chosen to satisfy

$$\frac{d\rho^{\rm eq}(\mathbf{x}_{\rm t},\mathbf{p}_{\rm t};t)}{dt} = 0, \tag{5}$$

then one reaches the equations of motion of ELD

$$\dot{\mathbf{x}} = \mathbf{M}^{-1}\mathbf{p}, \qquad \dot{\mathbf{p}} = -\frac{\partial {\rm V}_{\rm eff}^{\rm ELD}(\mathbf{x},\mathbf{p})}{\partial \mathbf{x}}, \tag{6}$$

with the effective force $-\frac{\partial {\rm V}_{\rm eff}^{\rm ELD}(\mathbf{x},\mathbf{p})}{\partial \mathbf{x}}$ given by

$$\frac{\partial \rho^{\rm eq}(\mathbf{x},\mathbf{p})}{\partial \mathbf{p}}\cdot\frac{\partial {\rm V}_{\rm eff}^{\rm ELD}(\mathbf{x},\mathbf{p})}{\partial \mathbf{x}} = \mathbf{p}^{\rm T}\mathbf{M}^{-1}\frac{\partial \rho^{\rm eq}(\mathbf{x},\mathbf{p})}{\partial \mathbf{x}}. \tag{7}$$

Here, $(\mathbf{x},\mathbf{p})$ is the phase point and $\rho^{\rm eq}(\mathbf{x},\mathbf{p})$ is the canonical distribution in the phase space. It is straightforward to show that the trajectory-based dynamics given by Eqs. (6) and (7) satisfies stationarity of the quantum canonical distribution function, i.e.,

$$\frac{\partial \rho^{\rm eq}(\mathbf{x},\mathbf{p};{\rm t})}{\partial {\rm t}} = 0. \tag{8}$$

Evaluation of the quantum correlation function Eq. (2) in the Wigner phase space with ELD[29,31] takes the expression

$$\begin{aligned} {\rm C}_{AB}(t) &= \frac{1}{\rm Z}\int d\mathbf{x}_0\int d\mathbf{p}_0\; A_W^{\beta}(\mathbf{x}_0,\mathbf{p}_0)B_W(\mathbf{x}_{\rm t},\mathbf{p}_{\rm t}) \\ &= \frac{1}{\rm Z}\int d\mathbf{x}_0\int d\mathbf{p}_0\; \rho_W^{eq}(\mathbf{x}_0,\mathbf{p}_0)f_{A^\beta}^W(\mathbf{x}_0,\mathbf{p}_0)B_W(\mathbf{x}_{\rm t},\mathbf{p}_{\rm t}), \end{aligned} \tag{9}$$

where A_W^{β}, B_W, and ρ_W^{eq} are the Wigner functions of the operators $\hat{A}^{\beta}$, $\hat{B}$, and $e^{-\beta\hat{H}}$, respectively. One sees that it takes the same procedure to express the functions $f_{A^\beta}^W$ and B_W as is often done in the Wigner phase space for the LSC-IVR/classical Wigner model.[11] The only difference between ELD and the LSC-IVR/classical Wigner model is that the trajectory $(\mathbf{x}_{\rm t},\mathbf{p}_{\rm t})$ of the latter always follows classical dynamics rather than Eq. (6). Since Eqs. (5) and (8) hold in ELD, time-averaging Eq. (9) leads to

$$\begin{aligned} C_{AB}(t) &= \frac{1}{T_0}\int_0^{T_0} dt'\langle A(t')B(t'+t)\rangle \\ &= \frac{1}{\rm Z}\int d\mathbf{x}_0\int d\mathbf{p}_0\;\rho^{eq}(\mathbf{x}_0,\mathbf{p}_0) \\ &\quad\times\frac{1}{T_0}\int_0^{T_0} dt'\; f_{A^\beta}^W(\mathbf{x}_{t'},\mathbf{p}_{t'})B_W(\mathbf{x}_{t+t'},\mathbf{p}_{t+t'}). \end{aligned} \tag{10}$$

If the dynamics of system is ergodic, the correlation function can be evaluated by a long time trajectory, i.e., Eq. (10) is simplified as

$$C_{AB}(t) = \frac{1}{T_0}\int_0^{T_0} dt'\; f_{A^\beta}^W(\mathbf{x}_{t'},\mathbf{p}_{t'})B_W(\mathbf{x}_{t+t'},\mathbf{p}_{t+t'}). \tag{11}$$

B. Evaluation of the effective force

One can express $\rho^{\rm eq}(\mathbf{x},\mathbf{p})$ in the Wigner phase space with the local Gaussian approximation[11,30,32] as

$$\frac{1}{\rm Z}\rho_{\rm W}^{\rm eq}(\mathbf{x},\mathbf{p}) = \frac{1}{\rm Z}\langle\mathbf{x}|{\rm e}^{-\beta\hat{\rm H}}|\mathbf{x}\rangle\left(\frac{\beta}{2\pi}\right)^{\rm N/2}|{\rm det}(\mathbf{M}_{\rm therm})|^{-1/2}\times\exp\left[-\frac{\beta}{2}\mathbf{p}^{\rm T}\mathbf{M}_{\rm therm}^{-1}\mathbf{p}\right], \tag{12}$$

where the thermal mass matrix $\mathbf{M}_{\rm therm}$ is given by

$$\mathbf{M}_{\rm therm}^{-1}(\mathbf{x}) = \mathbf{M}^{-1/2}\mathbf{T}\mathbf{Q}(\mathbf{u})\mathbf{T}^{\rm T}\mathbf{M}^{-1/2}. \tag{13}$$

Here, $\mathbf{Q}(\mathbf{u})$ is the (diagonal) quantum correction factor matrix with the LGA ansatz[11] (also see the definition of $\mathbf{u}$ in Ref. 11), and $\mathbf{T}$ is an orthogonal matrix that transforms the mass-weighted Hessian matrix of the potential energy surface into a diagonal one. Using the relation (13) or

$$\frac{\langle\mathbf{x}-\frac{\Delta\mathbf{x}}{2}|\,{\rm e}^{-\beta\hat{H}}\,|\mathbf{x}+\frac{\Delta\mathbf{x}}{2}\rangle}{\langle\mathbf{x}|{\rm e}^{-\beta\hat{H}}|\mathbf{x}\rangle} = \exp\left[-\frac{\Delta\mathbf{x}^{\rm T}\mathbf{M}_{\rm therm}(\mathbf{x})\Delta\mathbf{x}}{2\hbar^2\beta}\right], \tag{14}$$

it is straightforward to follow the same procedure for the LSC-IVR/classical Wigner model as shown in Ref. 11 to express the correlation function in the Wigner phase space [i.e., obtain the function $f_{A^\beta}^W(\mathbf{x},\mathbf{p})$ in Eq. (9)].

The ELD effective force defined by Eq. (7) with the density distribution Eq. (12) is

$$\begin{aligned} &-\frac{\partial}{\partial\mathbf{x}}{\rm V}_{\rm eff}^{\rm ELD}(\mathbf{x},\mathbf{p}) \\ &= \frac{1}{\beta}\mathbf{M}_{\rm therm}\mathbf{M}^{-1}\frac{\partial}{\partial\mathbf{x}}\ln\rho_W^{\rm eq}(\mathbf{x},\mathbf{p}) \\ &= \mathbf{M}_{\rm therm}\mathbf{M}^{-1}\left(\frac{1}{\beta}\frac{\partial}{\partial\mathbf{x}}\ln\langle\mathbf{x}|{\rm e}^{-\beta\hat{H}}|\mathbf{x}\rangle - \frac{1}{2}\mathbf{p}^{\rm T}\frac{\partial\mathbf{M}_{\rm therm}^{-1}(\mathbf{x})}{\partial\mathbf{x}}\mathbf{p}\right. \\ &\quad\left. -\frac{1}{2\beta}\frac{\partial}{\partial\mathbf{x}}\ln|{\rm det}(\mathbf{M}_{\rm therm})|\right). \end{aligned} \tag{15}$$

While several methodologies[29,31,32] have been proposed for evaluating Eq. (15), imaginary time path integral techniques[33–40] can also be implemented for ELD. Below we show how such an efficient path integral presentation of ELD can be constructed.

If a system is harmonic, it is trivial to show

$$\mathbf{M}_{\rm therm}(\mathbf{x}) \equiv \mathbf{M}_{\rm therm} = \beta\langle\mathbf{p}\mathbf{p}^{\rm T}\rangle, \tag{16}$$

where $\langle \mathbf{p}\mathbf{p}^{\mathrm{T}} \rangle$ is the canonical ensemble average of the covariance matrix of the momentum vector, which is *independent* of the position $\mathbf{x}$. If the thermal mass matrix $\mathbf{M}_{\mathrm{therm}}$ of Eq. (12) is defined by Eq. (16) for general systems [i.e., replacing the local Gaussian momentum approximation by a global one], the ELD effective force [Eq. (15)] can be simplified as

$$-\frac{\partial}{\partial \mathbf{x}} \mathrm{V}_{\mathrm{eff}}^{\mathrm{ELD}}(\mathbf{x}, \mathbf{p}) = \frac{1}{\beta} \mathbf{M}_{\mathrm{therm}} \mathbf{M}^{-1} \frac{\partial}{\partial \mathbf{x}} \ln \langle \mathbf{x} | \mathrm{e}^{-\beta \hat{\mathrm{H}}} | \mathbf{x} \rangle. \quad (17)$$

Equation (17) provides a numerically more favorable form for evaluating the effective force of the equations of motion of Eq. (6). Note that the covariance matrix $\langle \mathbf{p}\mathbf{p}^{\mathrm{T}} \rangle$ of Eq. (16) can be always efficiently evaluated by path integral techniques[33–41] before Eqs. (12) and (17) are employed in ELD. Evaluation of the thermal mass matrix $\mathbf{M}_{\mathrm{therm}}$ as defined by Eq. (16) does not request any specific form of the potential energy surface and takes the similar procedure as we estimate thermodynamic properties such as the kinetic energy.

It is straightforward to see that ELD with the quantum canonical distribution $\rho^{\mathrm{eq}}(\mathbf{x}, \mathbf{p})$ given by Eqs. (12) and (16) still rigorously satisfies the two important properties discussed in Sec. I. Note that the thermal mass matrix $\mathbf{M}_{\mathrm{therm}}$ defined by the quantum canonical distribution $\rho^{\mathrm{eq}}(\mathbf{x}, \mathbf{p})$ is often different from the (diagonal) physical mass matrix $\mathbf{M}$ except in the high temperature or classical limit.

III. PATH INTEGRAL REPRESENTATION OF EQUILIBRIUM LIOUVILLE DYNAMICS

For simplicity, we choose the 1-dim case for demonstration below. Inserting path integral beads in Eq. (12) leads to

$$\begin{aligned}
&\frac{1}{Z} \rho_{\mathrm{W}}^{\mathrm{eq}}(\mathrm{x}, \mathrm{p}) \\
&\overset{\mathrm{x}_1 \equiv \mathrm{x},\ \mathrm{p}_1 \equiv \mathrm{p}}{=} \lim_{\mathrm{P} \to \infty} \frac{1}{\mathrm{Z}} \left(\frac{MP}{2\pi\beta\hbar^2} \right)^{\mathrm{P}/2} \int \mathrm{dx}_2 \ldots \int \mathrm{dx}_{\mathrm{P}} \\
&\quad \times \exp\left\{ -\frac{\mathrm{PM}}{2\beta\hbar^2} [(\mathrm{x}_1 - \mathrm{x}_2)^2 + \cdots + (\mathrm{x}_{\mathrm{P}} - \mathrm{x}_1)^2] \right\} \\
&\quad \times \exp\left\{ -\frac{\beta}{\mathrm{P}} [\mathrm{V}(\mathrm{x}_1) + \cdots + \mathrm{V}(\mathrm{x}_{\mathrm{P}})] \right\} \\
&\quad \times \left(\frac{\beta}{2\pi} \right)^{1/2} |\mathbf{M}_{\mathrm{therm}}|^{-1/2} \exp\left[-\frac{\beta}{2} \mathrm{p}_1^{\mathrm{T}} \mathbf{M}_{\mathrm{therm}}^{-1} \mathrm{p}_1 \right], \quad (18)
\end{aligned}$$

where P is the number of path integral beads. Here, one sees that the samplings of the path integral beads $(\mathrm{x}_2, \ldots, \mathrm{x}_{\mathrm{P}})$ have to be completed in order to implement ELD in Eq. (6) with the effective force given by Eq. (17).

Consider the staging transformation[42,43]

$$\begin{aligned}
\xi_1 &= x_1, \\
\xi_{\mathrm{i}} &= x_{\mathrm{i}} - \frac{(\mathrm{i}-1)x_{\mathrm{i}+1} + x_1}{\mathrm{i}} \qquad (\mathrm{i} = \overline{2, \mathrm{P}}).
\end{aligned} \quad (19)$$

Its inverse transformation takes the following convenient recursive form:

$$\begin{aligned}
x_1 &= \xi_1, \\
x_{\mathrm{i}} &= \xi_{\mathrm{i}} + \frac{\mathrm{i}-1}{\mathrm{i}} x_{\mathrm{i}+1} + \frac{1}{\mathrm{i}} \xi_1 \quad (\mathrm{i} = \overline{2, \mathrm{P}}).
\end{aligned} \quad (20)$$

Here, $x_{P+1} \equiv x_1$. If one defines

$$\omega_P = \frac{\sqrt{P}}{\beta\hbar}, \quad (21)$$

Eq. (18) becomes

$$\begin{aligned}
&\frac{1}{Z} \rho_W^{eq}(x, p) \\
&\overset{\xi_1 \equiv x_1 \equiv x,\ p_1 \equiv p}{=} \lim_{P \to \infty} \frac{1}{Z} \left(\frac{MP}{2\pi\beta\hbar^2} \right)^{P/2} \int \mathrm{d}\xi_2 \cdots \int \mathrm{d}\xi_{\mathrm{P}} \\
&\quad \times \exp\left\{ -\beta \sum_{\mathrm{j}=1}^{\mathrm{P}} \left[\frac{1}{2} \bar{m}_j \omega_P^2 \xi_{\mathrm{j}}^2 + \frac{1}{P} V(x_{\mathrm{j}}(\xi_1, \ldots, \xi_{\mathrm{P}})) \right] \right\} \\
&\quad \times \left(\frac{\beta}{2\pi} \right)^{1/2} |\mathbf{M}_{\mathrm{therm}}|^{-1/2} \exp\left[-\frac{\beta}{2} p_1^{\mathrm{T}} \mathbf{M}_{\mathrm{therm}}^{-1} p_1 \right], \quad (22)
\end{aligned}$$

with the masses given by

$$\begin{aligned}
\bar{m}_1 &= 0, \\
\bar{m}_i &= \frac{i}{i-1} M \quad (i = \overline{2, P}).
\end{aligned} \quad (23)$$

One sees that all the staging variables $(\xi_2, \ldots, \xi_P)$ have the same frequency and all the fictitious masses $(\bar{m}_2, \ldots, \bar{m}_P)$ are in the same scale. If one defines

$$\phi(\xi_1, \ldots, \xi_P) = \frac{1}{P} \sum_{j=1}^{P} V(x_j(\xi_1, \ldots, \xi_P)), \quad (24)$$

then one obtains the chain rule

$$\begin{aligned}
\frac{\partial \phi}{\partial \xi_1} &= \sum_{i=1}^{P} \frac{\partial \phi}{\partial x_i} = \frac{1}{P} \sum_{i=1}^{P} V'(x_i), \\
\frac{\partial \phi}{\partial \xi_j} &= \frac{\partial \phi}{\partial x_j} + \frac{j-2}{j-1} \frac{\partial \phi}{\partial \xi_{j-1}}, \quad (j = \overline{2, P}),
\end{aligned} \quad (25)$$

from Eqs. (19) and (20). Therefore, one can employ such as the staging Monte Carlo approach[33,34,42] to efficiently evaluate the ELD effective force [Eq. (17)] from the following formula:

$$\begin{aligned}
-\frac{1}{\beta} \frac{\partial}{\partial x} \ln \rho_W^{eq}(x, p) &= -\frac{1}{\beta} \frac{\partial}{\partial x} \ln \langle x | e^{-\beta \hat{H}} | x \rangle \\
&\overset{\xi_1 \equiv x_1 \equiv x,\ p_1 \equiv p}{=} \frac{\lim_{\mathrm{P} \to \infty} \left(\frac{MP}{2\pi\beta\hbar^2} \right)^{P/2} \int d\xi_2 \cdots \int d\xi_P \exp\left\{ -\beta \sum_{j=2}^{P} \left[\frac{1}{2} \bar{\mathrm{m}}_{\mathrm{j}} \omega_{\mathrm{P}}^2 \xi_j^2 + \phi(\xi_1, \ldots, \xi_P) \right] \right\} \frac{1}{P} \sum_{j=1}^{P} V'(x_j)}{\lim_{\mathrm{P} \to \infty} \left(\frac{MP}{2\pi\beta\hbar^2} \right)^{P/2} \int d\xi_2 \cdots \int d\xi_P \exp\left\{ -\beta \sum_{j=2}^{P} \left[\frac{1}{2} \bar{\mathrm{m}}_{\mathrm{j}} \omega_{\mathrm{P}}^2 \xi_j^2 + \phi(\xi_1, \ldots, \xi_P) \right] \right\}}.
\end{aligned} \quad (26)$$

The real time propagation of the phase variables $(x,\ p) \equiv (\xi_1,\ p_1)$ [defined by the ELD equations of motions Eq. (6)] then involves an integral over $(\xi_2,\ \ldots,\ \xi_P)$ to evaluate at every time step. Below we introduce an efficient sampling of all variables in a molecular dynamics scheme.

Taking advantage of the isomorphism strategy proposed by Chandler and Wolynes,[44] one can insert fictitious momenta $(p_2,\ \ldots,\ p_P)$ into Eq. (22) or Eq. (26). For instance, Eq. (22) becomes

$$\begin{aligned}
&\frac{1}{Z}\rho_W^{\rm eq}(x,\ p)\\
&\overset{\xi_1\equiv x,\ p_1\equiv p}{=} \lim_{P\to\infty}\frac{1}{Z}\left(\frac{MP}{2\pi\beta\hbar^2}\right)^{P/2}\\
&\quad\times\int d\xi_2\cdots\int d\xi_P\int dp_2\cdots\int dp_P\\
&\quad\times\exp\left\{-\beta\left[\sum_{j=2}^{P}\frac{1}{2}\tilde{m}_j\omega_P^2\xi_j^2+\phi(\xi_1,\ldots,\xi_P)\right]\right\}\\
&\quad\times\left(\prod_{j=2}^{P}\frac{\beta}{2\pi\tilde{m}_j}\right)^{1/2}\exp\left\{-\beta\sum_{j=2}^{P}\frac{p_j^2}{2\tilde{m}_j}\right\}\\
&\quad\times\left(\frac{\beta}{2\pi}\right)^{1/2}|M_{\rm therm}|^{-1/2}\exp\left[-\frac{\beta}{2}p_1^{\rm T}M_{\rm therm}^{-1}p_1\right].
\end{aligned}\tag{27}$$

If one chooses the corresponding fictitious masses $(\tilde{m}_2,\ \ldots,\ \tilde{m}_P)$ as

$$\tilde{m}_i=\gamma_{ad}\bar{m}_i\qquad(i=\overline{2,\ P})\tag{28}$$

with $\gamma_{\rm ad}\in(0,\ 1]$ as an adiabatic parameter, and also defines the adiabatic frequencies $\omega_{\rm ad}$ as

$$\omega_{ad}=\omega_P/\sqrt{\gamma_{ad}},\tag{29}$$

Eq. (27) then becomes

$$\begin{aligned}
&\frac{1}{Z}\rho_W^{\rm eq}(x,\ p)\\
&\overset{\xi_1\equiv x,\ p_1\equiv p}{=} \lim_{P\to\infty}\frac{1}{Z}\left(\frac{MP}{2\pi\beta\hbar^2}\right)^{P/2}\\
&\quad\times\int d\xi_2\cdots\int d\xi_P\int dp_2\cdots\int dp_P\\
&\quad\times\exp\left\{-\beta\left[\sum_{j=2}^{P}\frac{1}{2}\tilde{m}_j\omega_{ad}^2\xi_j^2+\phi(\xi_1,\ldots,\xi_P)\right]\right\}\\
&\quad\times\left(\prod_{j=2}^{P}\frac{\beta}{2\pi\tilde{m}_j}\right)^{1/2}\exp\left\{-\beta\sum_{j=2}^{P}\frac{p_j^2}{2\tilde{m}_j}\right\}\\
&\quad\times\left(\frac{\beta}{2\pi}\right)^{1/2}|M_{\rm therm}|^{-1/2}\exp\left[-\frac{\beta}{2}p_1^{\rm T}M_{\rm therm}^{-1}p_1\right].
\end{aligned}\tag{30}$$

One sees that all the staging variables $(\xi_2,\ \ldots,\ \xi_P)$ share the same time scale that can be *well separated* from the time scale of $\xi_1\equiv x$ with the choice of the adiabatic parameter γ_{ad}. When the separation of time scales holds, one can define the following density distribution function:

$$\begin{aligned}
&\frac{1}{Z}\rho_W^{eq}(\xi_1,\ldots,\xi_P,\ p_1,\ldots,\ p_P)\\
&\overset{\xi_1\equiv x,\ p_1\equiv p}{=}\frac{1}{Z}\left(\frac{MP}{2\pi\beta\hbar^2}\right)^{P/2}\\
&\quad\times\left(\prod_{j=2}^{P}\frac{\beta}{2\pi\tilde{m}_j}\right)^{1/2}\exp\left\{-\beta\sum_{j=2}^{P}\frac{p_j^2}{2\tilde{m}_j}\right\}\\
&\quad\times\left(\frac{\beta}{2\pi}\right)^{1/2}|M_{\rm therm}|^{-1/2}\exp\left[-\frac{\beta}{2}p_1^{\rm T}M_{\rm therm}^{-1}p_1\right]\\
&\quad\times\exp\left\{-\beta\left[\sum_{j=2}^{P}\frac{1}{2}\tilde{m}_j\omega_{ad}^2\xi_j^2+\phi(\xi_1,\ldots,\xi_P)\right]\right\}
\end{aligned}\tag{31}$$

with the physical mass M for the physical phase space variables $(\xi_1,\ p_1)\equiv(x,\ p)$ and the fictional masses $\tilde{m}_j$ given in Eq. (28) for the other variables $(\xi_j,\ p_j)$, then the ELD equations of motion [Eqs. (6) and (7)] lead to

$$\begin{aligned}
\dot{\xi}_1&\equiv\dot{x}_1\equiv\dot{x}=\mathrm{M}^{-1}p,\\
\dot{p}_1&\equiv\dot{p}=-\mathrm{M}_{\rm therm}\mathrm{M}^{-1}\frac{\partial\phi}{\partial\xi_1}\\
&=-\mathrm{M}_{\rm therm}\mathrm{M}^{-1}\left(\frac{1}{P}\sum_{j=1}^{P}\frac{\partial V(x_j)}{\partial x_j}\right),\\
\dot{\xi}_j&=\tilde{m}_j^{-1}\ p_j,\\
\dot{p}_j&=-\tilde{m}_j\omega_{ad}^2\xi_j-\ \frac{\partial\phi}{\partial\xi_j}\quad(j=\overline{2,\ P}).
\end{aligned}\tag{32}$$

In order to ensure a proper canonical distribution for $(\xi_2,\ \ldots,\ \xi_P,\ p_2,\ \ldots,\ p_P)$, the equations of motion for $(\xi_2,\ \ldots,\ \xi_P,\ p_2,\ \ldots,\ p_P)$ in Eq. (32) must be coupled to a thermostatting method, such as Anderson themostat,[45] Nosé-Hoover chain,[46] generalized Gaussian moment,[47] or Langevin dynamics,[39,48] etc. Note that the quantum phase space variables $(\xi_1,\ p_1)\equiv(x,\ p)$ should *not* be coupled to a thermostatting method. When the adiabatic parameter $\gamma_{ad}\to 0$, Eq. (32) approaches the full adiabatic version of the path integral representation of ELD in the Wigner phase space, otherwise the partially adiabatic version of ELD is actually obtained, which could be more efficient. We note the path integral representation as path integral Liouville dynamics (PILD) in the paper. Fig. 1 provides a scheme representation of PILD.

One sees that PILD is reminiscent of the staging path integral molecular dynamics (PIMD) of Tuckerman *et al.*[38,43] when the following three conditions are satisfied:

(1) The variables $(\xi_1,\ p_1)\equiv(x,\ p)$ are also coupled to a thermostatting method.
(2) The thermal mass $\mathrm{M}_{\rm therm}$ is reduced to the mass of the system.
(3) The adiabatic parameter γ_{ad} is chosen as 1.

It is trivial to further show that all thermodynamic properties can be exactly obtained in PILD in the same spirit as done in the staging PIMD, as long as the first condition

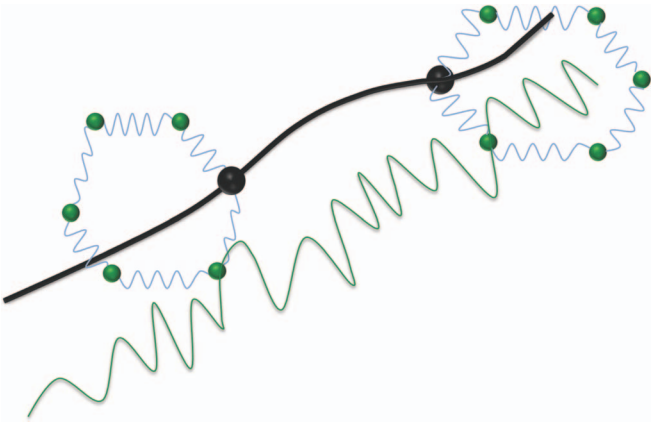

FIG. 1. Schematic representation of the PILD model. Imaginary time path integral beads and their interactions are depicted by a ring polymer as often done in PIMD. PILD chooses one of the path integral beads (in black) to construct the quantum phase space (**x**,**p**) where all dynamical properties and correlation functions are expressed. The fictional dynamics of the other path integral beads (in green) are treated in a similar way to the conventional PIMD, the purpose of which is only to generate the configurational average of Eq. (26) for evaluating the effective force on the fly.

is satisfied. More importantly, PILD offers an approach for calculating dynamical properties and real time correlation functions.

As the relation between ELD and CMD has been discussed in Ref. 30, it is also interesting to compare PILD to the path integral version of CMD.[23,49] While the former employs the staging transformation of the imaginary time path integral beads, the latter often uses the normal-mode transformation instead. CMD expresses the thermal correlation function with the position and momentum of the centroid of the path integral beads, and fails to give the correct result if both operators [$\hat{A}$ and $\hat{B}$ in Eq. (1)] are nonlinear operators, even for a harmonic potential.[31,32,50–54] As comparison, PILD expresses the thermal correlation function with Eq. (9) in the Wigner phase space that consists of the position of a path integral bead and its corresponding momentum, and treats both linear and *nonlinear* operators equally well.

IV. ANOTHER DERIVATION FROM EQUILIBRIUM HAMILTONIAN DYNAMICS

One can follow Ref. 32 to make a change of variables in Eq. (31)

$$p_{\rm eff} = {\rm M}_{\rm eff}{\rm M}^{-1} p \tag{33}$$

with the effective mass defined as

$${\rm M}_{\rm eff} = {\rm M}\,{\rm M}_{\rm therm}^{-1}{\rm M}. \tag{34}$$

When the thermal mass $\rm M_{therm}$ is given by Eq. (16), the effective mass $\rm M_{eff}$ is independent of the position. In such a case, it is clear from Ref. 32 that ELD can be closely related to EHD in phase space formulations of quantum mechanics, as we also show below.

The transformation of Eq. (33) gives the determinant of the Jacobian matrix as

$$\frac{\partial(\xi_1, \xi_2, \ldots, \xi_P, p_{\rm eff}, p_2, \ldots, p_P)}{\partial(\xi_1, \xi_2, \ldots, \xi_P, p_1, p_2, \ldots, p_P)} = |{\rm M}_{\rm eff}\,{\rm M}^{-1}| = |{\rm M}\,{\rm M}_{\rm therm}^{-1}|. \tag{35}$$

Here, $\xi_1 \equiv x$. The phase space distribution function with the new variables $(\xi_1, \xi_2, \ldots, \xi_P, p_{\rm eff}, p_2, \ldots, p_P)$ thus takes the form

$$\rho^{\rm eq}_{{\rm eff},\,W}(\xi_1, \ldots, \xi_P, p_{\rm eff}, p_2, \ldots, p_P) = |{\rm M}_{\rm therm}{\rm M}^{-1}|\rho^{eq}_W(\xi_1, \ldots, \xi_P, p_1, p_2, \ldots, p_P). \tag{36}$$

Equations (31) and (36) lead to

$$\frac{1}{Z}\rho^{eq}_{{\rm eff},\,W}(\xi_1, \ldots, \xi_P, p_{\rm eff}, p_2, \ldots, p_P) = \frac{1}{Z}\left(\frac{MP}{2\pi\beta\hbar^2}\right)^{P/2}\left(\prod_{j=2}^{P}\frac{\beta}{2\pi\tilde{m}_j}\right)^{1/2}\left(\frac{\beta}{2\pi}\right)^{1/2}|{\rm M}_{\rm eff}|^{-1/2} \times e^{-\beta H^{staging}_{\rm eff}(\xi_1,\xi_2,\ldots,\xi_P,p_{\rm eff},p_2,\ldots,p_P)} \tag{37}$$

with the effective staging Hamiltonian $H^{staging}_{\rm eff}$ defined as

$$H^{staging}_{\rm eff}(\xi_1, \xi_2, \ldots, \xi_P, p_{\rm eff}, p_2, \ldots, p_P) = \frac{1}{2}p^T_{\rm eff}{\rm M}^{-1}_{\rm eff}p_{\rm eff} + \sum_{j=2}^{P}\frac{p_j^2}{2\tilde{m}_j} + \sum_{j=2}^{P}\frac{1}{2}\tilde{m}_j\omega_{ad}^2\xi_j^2 + \phi(\xi_1, \ldots, \xi_P). \tag{38}$$

The Hamilton equations of motion generated from the effective staging Hamiltonian $H^{staging}_{\rm eff}$ become

$$\begin{aligned}
\dot{\xi}_1 &\equiv \dot{x}_1 \equiv \dot{x} = {\rm M}^{-1}_{\rm eff}\,p_{\rm eff},\\
\dot{p}_{\rm eff} &= -\frac{\partial\phi}{\partial\xi_1} \equiv -\frac{1}{P}\sum_{j=1}^{P}\frac{\partial V(x_j)}{\partial x_j},\\
\dot{\xi}_j &= \tilde{m}_j^{-1}p_j,\\
\dot{p}_j &= -\tilde{m}_j\omega_{ad}^2\xi_j - \frac{\partial\phi}{\partial\xi_j} \quad (j = \overline{2, P}).
\end{aligned} \tag{39}$$

Equation (39) is identical to Eq. (32) by virtue of the transformation of Eqs. (33) and (34). Thus, one sees that PILD can also be viewed as a path integral representation of EHD[32] in the Wigner phase space.

Interestingly, the effective Hamiltonian Eq. (38) and the equations of motion (39) can be related to the adiabatic Wigner PIMD (AWPIMD) proposed by Martyna and Cao[55,56] nearly 20 years ago. (We were not aware of their work[55,56] when we were preparing the paper.) Nevertheless, the major differences between PILD and AWPIMD are

(1) PILD employs Eq. (9)—an exact mapping of the thermal correlation function in the Wigner phase space,[29,31] which leads to exact results in the harmonic limit for any time correlation functions even when nonlinear operators are involved. This is derived from Liouville's theorem in quantum mechanics (i.e., the Von Neumann

equation) for the generalized density operator $\hat{A}^{\beta}(t) = \frac{1}{Z} e^{-i\hat{H}t/\hbar}\hat{A}^{\beta}e^{i\hat{H}t/\hbar}$ as shown in Refs. 29 and 31. As comparison, the approach to evaluate the thermal correlation function in AWPIMD as explicitly discussed in Sec. II C of Ref. 56 does *not* guarantee exact results in the harmonic limit for correlation functions with any nonlinear operators.

(2) As pointed out by Martyna and Cao,[55,56] the effective masses of AWPIMD "must be introduced in an appropriate set of normal modes," which is not convenient to use for dynamics of molecular systems. The thermal mass matrix [Eq. (16)] or the effective mass matrix [Eq. (34)] introduced in PILD, however, is defined (and evaluated) in the Cartesian coordinates. As a result, PILD is much more convenient to use for general multi-dimensional systems.

V. NUMERICAL EXAMPLES

A. Algorithm for PILD with Langevin thermostat

In the paper, we employ a simple (white noise) Langevin dynamics[39,48] to thermostat the staging path integral variables $(\xi_2, \ldots, \xi_P, p_2, \ldots, p_P)$ in PILD. Equation (32) becomes

$$\begin{aligned}
\dot{\xi}_1 &\equiv \dot{x}_1 \equiv \dot{x} = \mathrm{M}^{-1} p, \\
\dot{p}_1 &\equiv \dot{p} = -\mathrm{M}_{\mathrm{therm}}\mathrm{M}^{-1}\frac{\partial \phi}{\partial \xi_1} \\
&= -\mathrm{M}_{\mathrm{therm}}\mathrm{M}^{-1}\left(\frac{1}{P}\sum_{j=1}^{P}\frac{\partial V(x_j)}{\partial x_j}\right), \qquad (40)\\
\dot{\xi}_j &= \tilde{m}_j^{-1}\, p_j, \\
\dot{p}_j &= -\tilde{m}_j\omega_{ad}^2\xi_j - \frac{\partial \phi}{\partial \xi_j} - \gamma_{Lang}\, p_j \\
&\quad + \sqrt{\frac{2\tilde{m}_j\gamma_{Lang}}{\beta}}\,\eta_j(t) \quad (j = \overline{2, P}),
\end{aligned}$$

where $\eta_j(t)$ is an independent Gaussian-distributed random number with zero mean and unit variance [$\langle\eta_j(t)\rangle = 0$ and $\langle\eta_j(t)\eta_j(t')\rangle = \delta(t - t')$], which is different for each physical degree of freedom, each staging mode ($j = \overline{2, P}$), and each time step. The Langevin friction coefficient γ_{Lang} is the same for all staging modes ($j = \overline{2, P}$) because they share the same frequency ω_{ad}.

When the system is a free particle, the Langevin dynamics of each staging mode ($j = \overline{2, P}$) reduces to that of a harmonic oscillator with the frequency ω_{ad}, i.e.,

$$\begin{aligned}
\dot{\xi}_j &= \tilde{m}_j^{-1}\, p_j, \\
\dot{p}_j &= -\tilde{m}_j\omega_{ad}^2\xi_j - \gamma_{Lang}\, p_j \\
&\quad + \sqrt{\frac{2\tilde{m}_j\gamma_{Lang}}{\beta}}\,\eta_j(t) \quad (j = \overline{2, P}).
\end{aligned} \qquad (41)$$

Following Refs. 39 and 57, one can choose the Langevin friction coefficient γ_{Lang} as

$$\gamma_{Lang}^{opt} = 2\omega_{ad} \qquad (42)$$

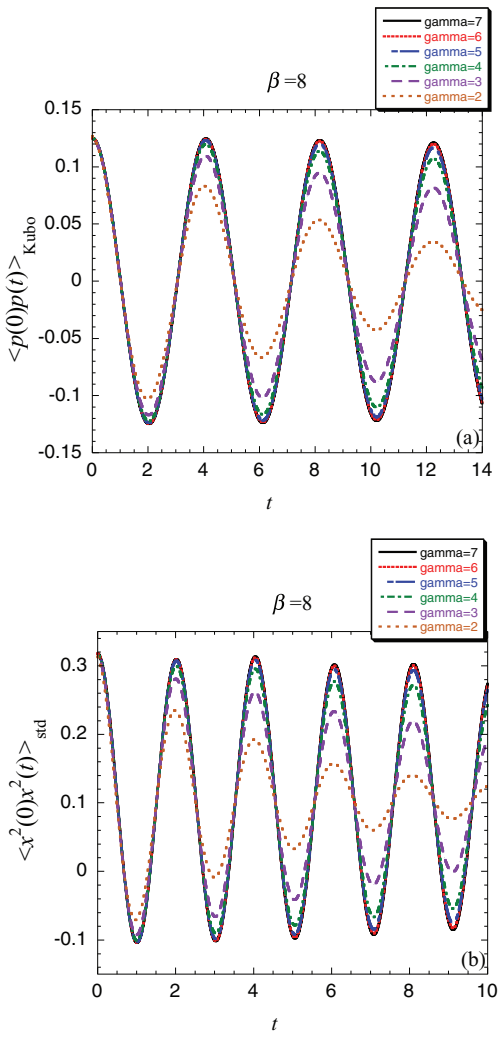

FIG. 2. (a) and (b) The PILD autocorrelation functions for the one-dimensional anharmonic oscillator for $\beta = 8$ with the choice of the adiabatic parameter $\gamma_{\mathrm{ad}} = 10^{-\mathrm{gamma}}$. Fully converged results are obtained with gamma = 6 for the system.

that gives the smallest relevant autocorrelation time of the harmonic oscillator Hamiltonian

$$\tilde{H} = \frac{p_j^2}{2\tilde{m}_j} + \frac{1}{2}\tilde{m}_j\omega_{ad}^2\xi_j^2. \qquad (43)$$

Note that the autocorrelation time

$$\tau_{\tilde{H}} = \frac{1}{\langle\tilde{H}^2\rangle - \langle\tilde{H}\rangle^2}\int_0^{\infty} dt\langle(\tilde{H}(0) - \langle\tilde{H}\rangle)(\tilde{H}(t) - \langle\tilde{H}\rangle)\rangle \qquad (44)$$

is[57]

$$\tau_{\tilde{H}} = \frac{1}{\gamma_{Lang}} + \frac{\gamma_{Lang}}{4\omega_{ad}^2} \qquad (45)$$

for the Langevin dynamics in Eq. (41). So Eq. (42) is suggested as the optimum value of Langevin friction coefficient γ_{Lang} in Eq. (40) for PILD because it is expected to offer the most efficient sampling for the staging path integral variables $(\xi_2, \ldots, \xi_P)$ [in the free particle limit]. We will further demonstrate that the PILD result is *insensitive* to the choice of the friction coefficient γ_{Lang} around the optimum regime.

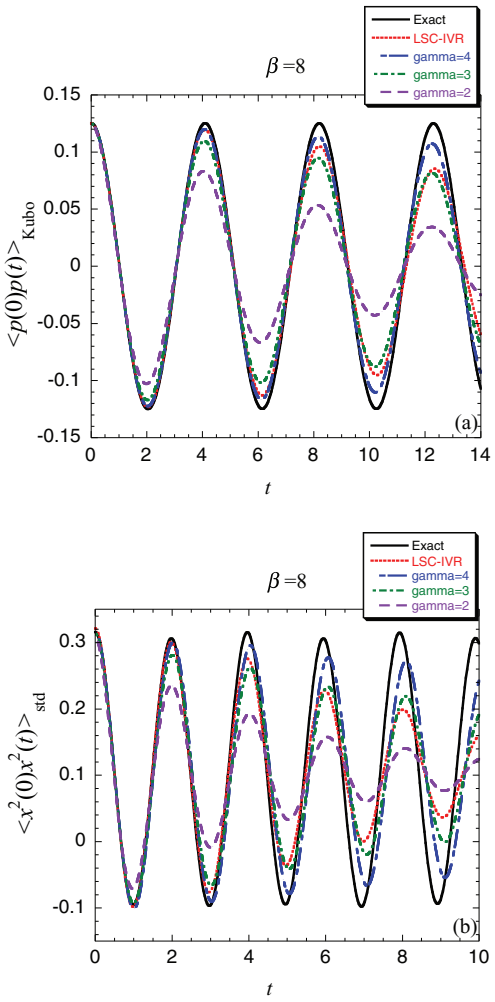

FIG. 3. (a) and (b) As in Fig. 2, but with comparison to the exact quantum correlation functions and the LSC-IVR results.

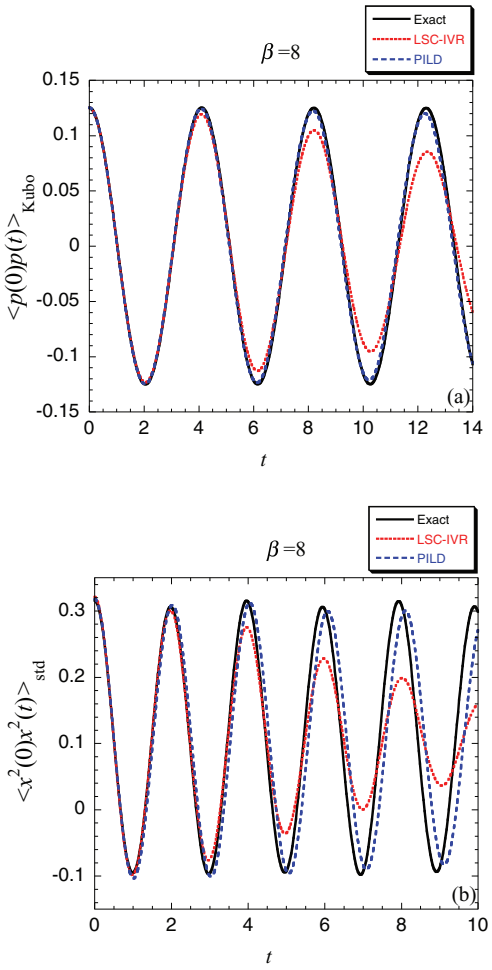

FIG. 4. (a) and (b) The converged PILD autocorrelation functions compared the LSC-IVR and exact quantum results for the one-dimensional anharmonic oscillator for $\beta = 8$.

The velocity Verlet algorithm can be constructed for integrating the equations of motion in Eq. (40) for PILD (as done for molecular dynamics by Bussi and Parrinello[48] and for PIMD by Ceriotti *et al.*[39]). Such an algorithm for propagating the PILD trajectory through a time interval Δt is as follows:

$$p_j \leftarrow c_1 p_j + c_2 \sqrt{\frac{\tilde{m}_j}{\beta}}\eta_j \quad (j = \overline{2, P}), \tag{46}$$

$$\begin{aligned} p_1 &\leftarrow p_1 - \mathrm{M_{therm}} \mathrm{M}^{-1} \frac{\partial \phi}{\partial \xi_1}\frac{\Delta t}{2}, \\ p_j &\leftarrow p_j - \frac{\partial \phi}{\partial \xi_j}\frac{\Delta t}{2} \quad (j = \overline{2, P}), \end{aligned} \tag{47}$$

$$\begin{aligned} &\xi_1 \leftarrow \xi_1 + \mathrm{M}^{-1} p_1 \Delta t \\ &\begin{pmatrix} \xi_j \\ p_j \end{pmatrix} \leftarrow \begin{pmatrix} \cos(\omega_{ad}\Delta t) & \sin(\omega_{ad}\Delta t)/\tilde{m}_j\omega_{ad} \\ -\tilde{m}_j\omega_{ad}\sin(\omega_{ad}\Delta t) & \cos(\omega_{ad}\Delta t) \end{pmatrix} \\ &\times \begin{pmatrix} \xi_j \\ p_j \end{pmatrix} \quad (j = \overline{2, P}), \end{aligned} \tag{48}$$

$$\begin{aligned} p_1 &\leftarrow p_1 - \mathrm{M_{therm}} \mathrm{M}^{-1} \frac{\partial \phi}{\partial \xi_1}\frac{\Delta t}{2}, \\ p_j &\leftarrow p_j - \frac{\partial \phi}{\partial \xi_j}\frac{\Delta t}{2} \quad (j = \overline{2, P}), \end{aligned} \tag{49}$$

$$p_j \leftarrow c_1 p_j + c_2 \sqrt{\frac{\tilde{m}_j}{\beta}}\eta_j \quad (j = \overline{2, P}). \tag{50}$$

Here, η_j is the independent Gaussian-distributed random number as discussed for Eq. (40), which is different for each invocation of Eq. (46) or Eq. (50), and the coefficients c_1 and c_2 are[39,48]

$$\begin{aligned} \mathrm{c}_1 &= \exp[-\gamma_{Lang}\Delta \mathrm{t}/2], \\ \mathrm{c}_2 &= \sqrt{1-(\mathrm{c}_1)^2}. \end{aligned} \tag{51}$$

While the forces in Eq. (47) are obtained from the previous time step, those in Eq. (49) at the current time step can be efficiently evaluated by the chain rule Eq. (25). One sees that the inverse staging transformation Eq. (20) is invoked only once [for Eq. (49)] in the integrator [Eqs. (46)–(50)] and the staging transformation Eq. (19) is not involved at all.

We note that Leimkuhler and Matthews[58,59] have recently investigated a few Langevin dynamics integrators, it will be

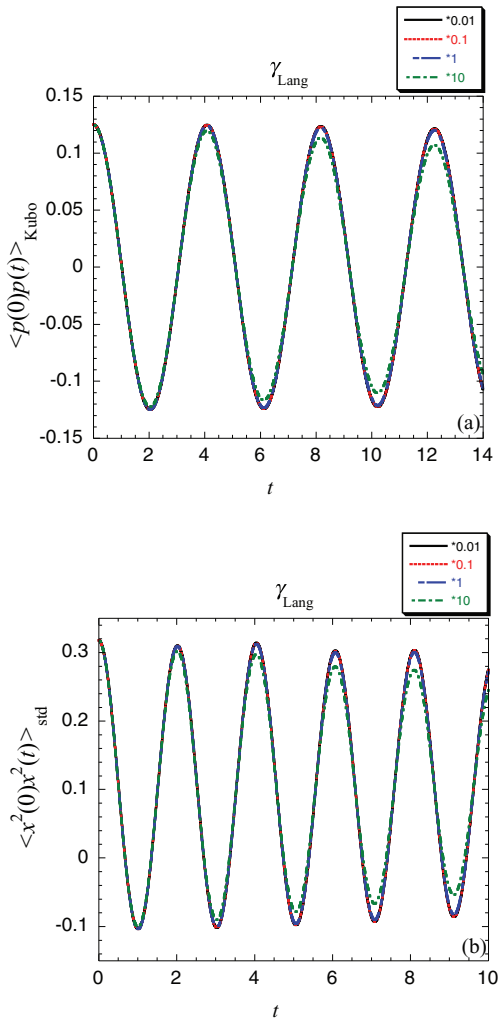

FIG. 5. (a) and (b) The PILD autocorrelation functions for the one-dimensional anharmonic oscillator for $\beta = 8$ with the choice of the friction coefficient $\gamma_{\rm Lang}$ when the Langevin thermostat is employed. Black solid line: $\gamma_{\rm Lang} = 0.01\ \gamma_{\rm Lang}^{\rm opt}$. Red dotted line: $\gamma_{\rm Lang} = 0.1\ \gamma_{\rm Lang}^{\rm opt}$. Blue short-long-dashed line: $\gamma_{\rm Lang} = \gamma_{\rm Lang}^{\rm opt}$. Green dotted-dashed line: $\gamma_{\rm Lang} = 10\ \gamma_{\rm Lang}^{\rm opt}$. (Here, the adiabatic parameter is $\gamma_{\rm ad} = 10^{-6}$.)

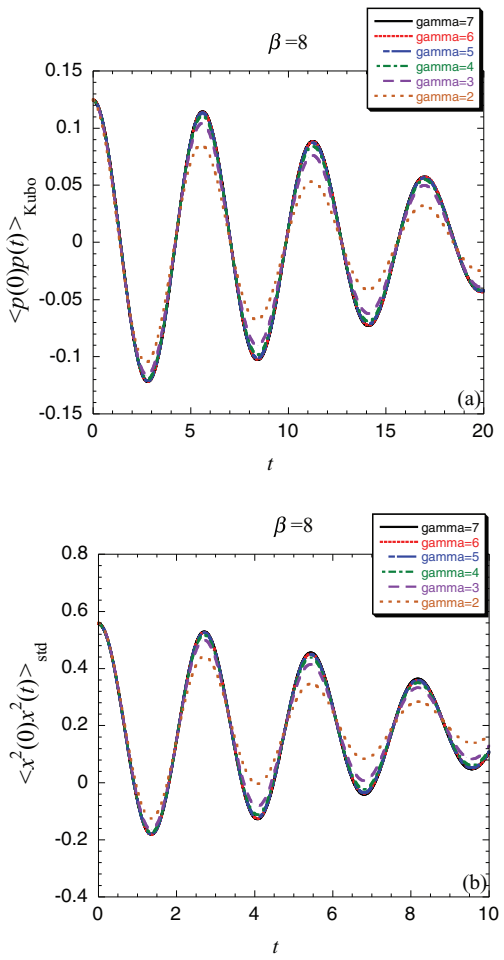

FIG. 6. (a) and (b) The PILD autocorrelation functions for the one-dimensional quartic oscillator for $\beta = 8$ with the choice of the adiabatic parameter $\gamma_{\rm ad} = 10^{-\rm gamma}$. Fully converged results are obtained with *gamma* = 6 for the system.

interesting to employ and test some of them (such as the BAOAB method) for PILD in the future.

B. Model tests

We consider two correlation functions $\langle p(0)p(\mathrm{t})\rangle_{\rm Kubo}$ and $\langle x^2(0)x^2(\mathrm{t})\rangle_{\rm std}$, with $\hat{A}^\beta = \hat{p}^\beta_{\rm Kubo}$ and $\hat{A}^\beta = \mathrm{e}^{-\beta\hat{H}}\hat{x}^2$ in Eq. (1), respectively. Expressing the correlation functions in the Wigner phase space [i.e., Eq. (9)] as is often done for the LSC-IVR/classical Wigner model[11] leads to

$$\mathrm{f}^W_{A^\beta}(x,\,p) = \mathrm{M}\,\mathrm{M}^{-1}_{\rm therm}p \tag{52}$$

for $\hat{A}^\beta = \hat{p}^\beta_{\rm Kubo}$ and

$$\mathrm{Re}\big[f^W_{A^\beta}(x,\,p)\big] = x^2 + \frac{\beta\hbar^2}{4}\mathrm{M}^{-1}_{\rm therm} - \frac{\beta^2\hbar^2}{4}(\mathrm{M}^{-1}_{\rm therm}p)^{\rm T}\mathrm{M}^{-1}_{\rm therm}p \tag{53}$$

for the real part for $\hat{A}^\beta = \mathrm{e}^{-\beta\hat{H}}\hat{x}^2$. The Wigner function $B_W(x,\,p)$ is the classical function (of $\hat{B}$) itself in either correlation function.

The two models are the asymmetric anharmonic potential

$$\mathrm{V(x)} = \frac{1}{2}\mathrm{M}\omega^2\mathrm{x}^2 - 0.10\mathrm{x}^3 + 0.10\mathrm{x}^4 \tag{54}$$

(with $\mathrm{M} = 1,\ \omega = \sqrt{2},$ and $\hbar = 1$) and a more severe model – the pure quartic well

$$\mathrm{V(x)} = \mathrm{x}^4/4 \tag{55}$$

(with $\mathrm{M} = 1$ and $\hbar = 1$). Since PILD approaches LSC-IVR in the high temperature limit, we focus on a low temperature $\beta = 8$. The exact quantum correlation functions and the LSC-IVR results have been presented for comparison.

Figs. 2–5 show the PILD results for the first model [Eq. (54)]. As seen in Fig. 2, converged correlation functions are obtained with $\gamma_{\rm ad} = 10^{-6}$ (with a time step $dt = 10^{-5} \sim 10^{-4}$). They match the exact quantum results almost perfectly, except a slight frequency shift and slight dephasing in the amplitude at long times as shown in Fig. 3. Both Figs. 2 and 3 demonstrate that the correlation function is in progressively better agreement with the quantum result at

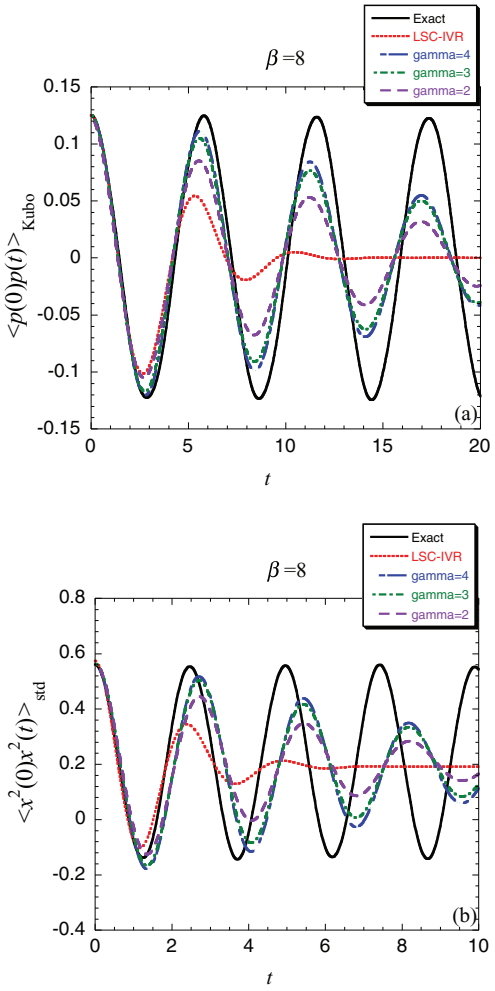

FIG. 7. (a) and (b) As in Fig. 6, but with comparison to the exact quantum correlation functions and the LSC-IVR results.

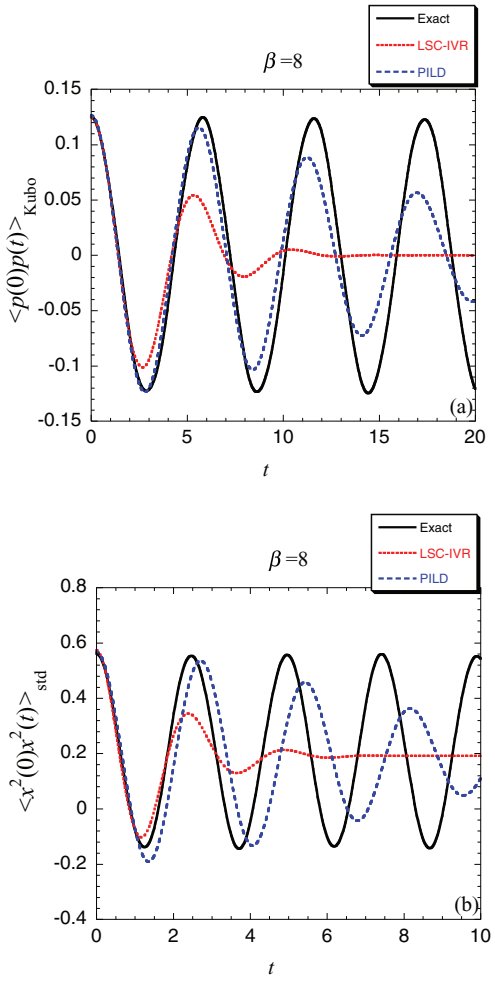

FIG. 8. (a) and (b) The converged PILD autocorrelation functions compared the LSC-IVR and exact quantum results for the one-dimensional quartic oscillator for $\beta = 8$.

longer times as the adiabatic parameter $\gamma_{\rm ad}$ decreases. Interestingly, Fig. 4 shows that PILD with even a relatively larger adiabatic parameter $\gamma_{\rm ad} = 10^{-3}$ or 10^{-4} (with a time step $dt \sim 10^{-3}$) is able to show systematical improvement over LSC-IVR at longer times. Fig. 5 shows how the PILD results change with the friction coefficient $\gamma_{\rm Lang}$ when PILD is employed with the Langevin thermostat. When $\gamma_{\rm Lang}$ is around the optimum value [Eq. (42)] or smaller, the PILD results are insensitive to the choice of the friction coefficient.

The PILD results for the pure quartic well [Eq. (55)] are demonstrated in Figs. 6–9. Figs. 6 and 7 show that the correlation function agrees increasingly better with the exact result at longer times as $\gamma_{\rm ad}$ decreases. Converged data are obtained with $\gamma_{\rm ad} = 10^{-6}$ (with a time step $dt = 10^{-5} \sim 10^{-4}$). The comparison with the exact results in Fig. 7 show that PILD describes the amplitude of oscillation reasonably well with a noticeable frequency shift after the first period, which significantly improves over LSC-IVR that shows too quick dephasing after one vibrational period. Fig. 8 further shows that systematical improvement over LSC-IVR at longer times can be achieved by PILD with even a relatively larger adiabatic parameter $\gamma_{\rm ad} = 10^{-2}$ or 10^{-3} (with a time step $dt \sim 10^{-3}$). Similar to Fig. 5, Fig. 9 also shows that the PILD correlation function is insensitive to the choice of the friction coefficient $\gamma_{\rm Lang}$ when it is around the suggested optimum value [Eq. (42)] or even smaller.

As comparison, it is well known that either CMD or RPMD works poorly for the correlation function of which both operators [$\hat{A}$ and $\hat{B}$ in Eq. (1)] are nonlinear operators.[31,32,50–54,60,61] For instance, Fig. 1 of Ref. 50, Fig. 1 of Ref. 31, and Fig. 1 of Ref. 32 demonstrate that neither CMD nor RPMD leads to correct results for $\langle x^2(0)x^2(t)\rangle_{\rm Kubo}$ even for a one-dimensional harmonic well. In addition to Fig. 5 of Ref. 60, Fig. 3 or Fig. 10 of Ref. 53 shows that CMD or RPMD produces poor results for $\langle x^2(0)x^2(t)\rangle_{\rm Kubo}$ for a one-dimensional anharmonic potential or the pure quartic well [Eq. (55)]. Since these results have already been demonstrated and discussed in the literature, we do not include them in the paper.

C. Discussion

It is shown that ELD[17,18] or EHD[32] fails to describe quantum recurrence/rephrasing effects, so does the PILD approach. However, long-time quantum recurrence/rephrasing effects (often shown in one-dimensional bounded systems) are anticipated to be quenched by coupling among the various

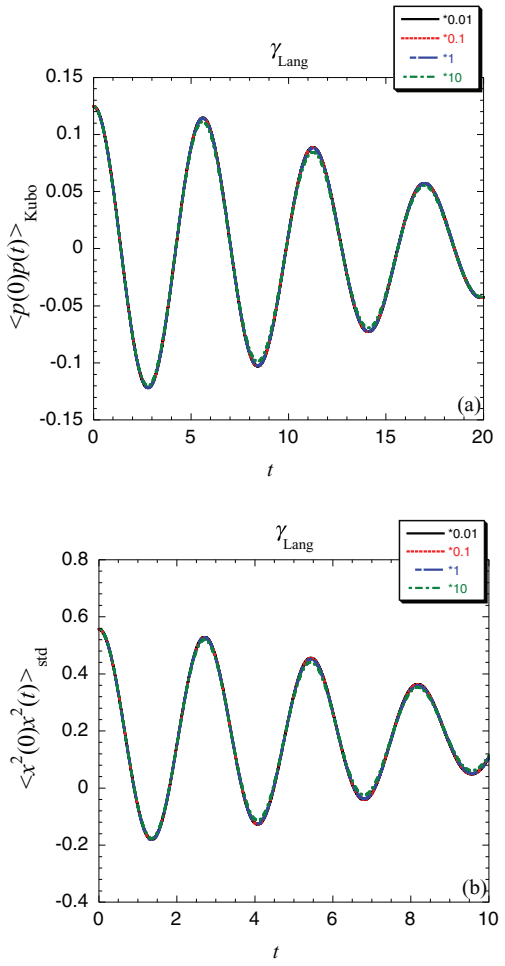

FIG. 9. (a) and (b) The PILD autocorrelation functions for the one-dimensional quartic oscillator for $\beta = 8$ with the choice of the friction coefficient γ_{Lang} when the Langevin thermostat is employed. Black solid line: $\gamma_{\text{Lang}} = 0.01\ \gamma_{\text{Lang}}^{\text{opt}}$. Red dotted line: $\gamma_{\text{Lang}} = 0.1\ \gamma_{\text{Lang}}^{\text{opt}}$. Blue short-long-dashed line: $\gamma_{\text{Lang}} = \gamma_{\text{Lang}}^{\text{opt}}$. Green dotted-dashed line: $\gamma_{\text{Lang}} = 10\ \gamma_{\text{Lang}}^{\text{opt}}$. (Here, the adiabatic parameter is $\gamma_{\text{ad}} = 10^{-6}$.)

degrees of freedom in condensed phase systems. As seen from the model tests (Figs. 2–9), PILD can accurately capture the most important short time dephasing behavior and extend the accuracy of correlation functions of both linear and *nonlinear* operators to longer time (comparing with LSC-IVR and other comparable methods). Because comparison of LSC-IVR to experiment has demonstrated that the physical decay often dominates in many condensed phase systems,[9–13,62–75] Figs. 4 and 8 imply that the PILD correlation function will converge much faster for these systems as the adiabatic parameter γ_{ad} decreases. Therefore, it can provide a practical and useful tool for including quantum effects for large/complex molecular systems in condensed phase.

When the simple (white noise) Langevin dynamics algorithm [Eqs. (46)–(50)] is used in PILD, it is shown that converged results can be efficiently obtained with the Langevin friction coefficient γ_{Lang} chosen as $2\omega_{\text{ad}}$ or slightly less. One can employ other thermostatting methods (such as Nosé-Hoover chain,[46] Anderson themostat,[45] generalized Gaussian moment,[47] etc.) as well for the staging path integral variables $(\xi_2, \ldots, \xi_P, p_2, \ldots, p_P)$ in PILD. It will be particularly interesting to see how the generalized Langevin equation with colored noise[39,40] can be implemented for the staging modes in PILD, as it has been shown that the generalized Langevin dynamics can offer an efficient sampling algorithm for PIMD when the normal mode transformation is employed.

VI. CONCLUSION REMARKS

In this paper, we present an imaginary time path integral based method for describing quantum dynamics effects. The method—PILD is derived from the path integral presentation of the ELD approach[30,31] in the molecular dynamics scheme. The staging transformation of the path integral beads is used to develop the method. Since implementation of PILD does not request any specific form of the potential energy surface, it offers a potentially useful approach for general condensed phase molecular systems to have the two important properties listed in Sec. I.

Finally, we note that both LSC-IVR and PILD produce exact correlation functions (of both linear and *nonlinear* operators) in the harmonic limit (i.e., the second property listed in Sec. I). While PILD conserves the mapping canonical density distribution (the first property listed in Sec. I), LSC-IVR preserves the mapping Hamiltonian (in the Wigner phase space) that is equivalent to the classical energy.[66] The former corresponds to the quantum commutation

$$[e^{-\beta\hat{H}}, e^{-i\hat{H}t/\hbar}] = 0, \tag{56}$$

and the latter is the counterpart of the commutation

$$[\hat{H}, \mathrm{e}^{-i\hat{H}t/h}] = 0. \tag{57}$$

It will be interesting in future work to test PILD for various correlation functions in condensed phase molecular systems, for which LSC-IVR/classical Wigner already works rather well for short time dynamics.[9–13,62–75] It would also certainly be of interest to compare PILD to other imaginary time path integral based methods such as CMD and RPMD for realistic molecular systems.

Note added in proof: In the reviewing process, we became aware of the work by Martyna and Cao[55,56] on the adiabatic Wigner PIMD. We thank the 1st referee for pointing it out.

ACKNOWLEDGMENTS

This work was supported by the National Science Foundation of China (NSFC) Grant No. 21373018 and by the Recruitment Program of Global Experts. We also acknowledge a generous allocation of supercomputing time from the National Energy Research Scientific Computing Center (NERSC) and the use of the computational cluster resources provided by the Beijing supercomputer center and by the Tianjing supercomputer center.

[1] W. H. Miller, Proc. Natl. Acad. Sci. U.S.A. **102**(19), 6660 (2005).
[2] W. H. Miller, J. Chem. Phys. **125**(13), 132305 (2006).
[3] G. A. Voth, Adv. Chem. Phys. **XCIII**, 135 (1996).

[4]S. Habershon, D. E. Manolopoulos, T. E. Markland, and T. F. Miller III, Annu. Rev. Phys. Chem. **64**, 387 (2013).
[5]E. Rabani and D. R. Reichman, Annu. Rev. Phys. Chem. **56**, 157 (2005).
[6]B. J. Berne and G. D. Harp, Adv. Chem. Phys. **17**, 63 (1970).
[7]R. Zwanzig, *Nonequilibrium Statistical Mechanics* (Oxford University Press, New York, 2001).
[8]D. A. McQuarrie, *Statistical Mechanics* (University Science Books, Sausalito, CA, 2000).
[9]H. Wang, X. Sun, and W. H. Miller, J. Chem. Phys. **108**(23), 9726 (1998).
[10]X. Sun, H. Wang, and W. H. Miller, J. Chem. Phys. **109**(17), 7064 (1998).
[11]J. Liu and W. H. Miller, J. Chem. Phys. **131**(7), 074113 (2009).
[12]Q. Shi and E. Geva, J. Phys. Chem. A **107**, 9059 (2003).
[13]J. A. Poulsen, G. Nyman, and P. J. Rossky, J. Chem. Phys. **119**(23), 12179 (2003).
[14]E. Pollak and J. L. Liao, J. Chem. Phys. **108**(7), 2733 (1998).
[15]R. Hernandez and G. A. Voth, Chem. Phys. **233**(2–3), 243 (1998).
[16]J. Shao and N. Makri, J. Phys. Chem. A **103**, 7753 (1999).
[17]J. Shao and N. Makri, J. Phys. Chem. A **103**, 9479 (1999).
[18]A. Nakayama and N. Makri, J. Chem. Phys. **119**, 8592 (2003).
[19]N. Makri, A. Nakayama, and N. Wright, J. Theor. Comput. Chem. **03**, 391 (2004).
[20]J. Liu and W. H. Miller, J. Chem. Phys. **125**(22), 224104 (2006).
[21]J. Cao and G. A. Voth, J. Chem. Phys. **99**(12), 10070 (1993).
[22]S. Jang and G. A. Voth, J. Chem. Phys. **111**, 2371 (1999).
[23]T. D. Hone, P. J. Rossky, and G. A. Voth, J. Chem. Phys. **124**(15), 154103 (2006).
[24]A. Witt, S. D. Ivanov, M. Shiga, H. Forbert, and D. Marx, J. Chem. Phys. **130**(19), 194510 (2009).
[25]I. R. Craig and D. E. Manolopoulos, J. Chem. Phys. **121**(8), 3368 (2004).
[26]B. J. Braams and D. E. Manolopoulos, J. Chem. Phys. **125**(12), 124105 (2006).
[27]J. O. Richardson and S. C. Althorpe, J. Chem. Phys. **131**(21), 214106 (2009).
[28]A. R. Menzeleev, F. Bell, and T. F. Miller III, J. Chem. Phys. **140**(6), 064103 (2014).
[29]J. Liu and W. H. Miller, J. Chem. Phys. **126**(23), 234110 (2007).
[30]J. Liu and W. H. Miller, J. Chem. Phys. **134**(10), 104101 (2011).
[31]J. Liu and W. H. Miller, J. Chem. Phys. **134**(10), 104102 (2011).
[32]J. Liu, J. Chem. Phys. **134**(19), 194110 (2011).
[33]D. M. Ceperley, Rev. Mod. Phys. **67**, 279 (1995).
[34]D. M. Ceperley and L. Mitas, Adv. Chem. Phys. **93**, 1 (1996).
[35]M. Parrinello and A. Rahman, J. Chem. Phys. **80**, 860 (1984).
[36]B. J. Berne and D. Thirumalai, Annu. Rev. Phys. Chem. **37**, 401 (1986).
[37]G. J. Martyna, A. Hughes, and M. E. Tuckerman, J. Chem. Phys. **110**(7), 3275 (1999).
[38]M. E. Tuckerman, in *Quantum Simulations of Complex Many-Body Systems: From Theory to Algorithms*, edited by J. Grotendorst, D. Marx, and A. Muramatsu (John von Neumann Institute for Computing, Jülich, 2002), Vol. 10, p. 269.
[39]M. Ceriotti, M. Parrinello, T. E. Markland, and D. E. Manolopoulos, J. Chem. Phys. **133**(12), 124104 (2010).
[40]M. Ceriotti, D. E. Manolopoulos, and M. Parrinello, J. Chem. Phys. **134**(8), 084104 (2011).
[41]M. Ceriotti and D. E. Manolopoulos, Phys. Rev. Lett. **109**(10), 100604 (2012).
[42]E. L. Pollock and D. M. Ceperley, Phys. Rev. B **30**(5), 2555 (1984).
[43]M. E. Tuckerman, B. J. Berne, G. J. Martyna, and M. L. Klein, J. Chem. Phys. **99**(4), 2796 (1993).
[44]D. Chandler and P. G. Wolynes, J. Chem. Phys. **74**, 4078 (1981).
[45]H. C. Andersen, J. Chem. Phys. **72**(4), 2384 (1980).
[46]G. J. Martyna, M. L. Klein, and M. Tuckerman, J. Chem. Phys. **97**, 2635 (1992).
[47]Y. Liu and M. E. Tuckerman, J. Chem. Phys. **112**(4), 1685 (2000).
[48]G. Bussi and M. Parrinello, Phys. Rev. E **75**(5), 056707 (2007).
[49]J. Cao and G. A. Voth, J. Chem. Phys. **101**(7), 6168 (1994).
[50]A. Horikoshi and K. Kinugawa, J. Chem. Phys. **122**(17), 174104 (2005).
[51]D. R. Reichman, P. N. Roy, S. Jang, and G. A. Voth, J. Chem. Phys. **113**(3), 919 (2000).
[52]T. D. Hone and G. A. Voth, J. Chem. Phys. **121**(13), 6412 (2004).
[53]F. Paesani and G. A. Voth, J. Chem. Phys. **129**(19), 194113 (2008).
[54]Q. Shi and E. Geva, J. Chem. Phys. **119**(17), 9030 (2003).
[55]J. Cao and G. J. Martyna, J. Chem. Phys. **104**(5), 2028 (1996).
[56]G. J. Martyna, J. Chem. Phys. **104**(5), 2018 (1996).
[57]C. W. Gardiner, *Handbook of Stochastic Methods: For Physics, Chemistry, and the Natural Sciences*, 2nd ed. (Springer-Verlag, Berlin, 1986).
[58]B. Leimkuhler and C. Matthews, J. Chem. Phys. **138**(17), 174102 (2013).
[59]B. Leimkuhler and C. Matthews, Appl. Math. Res. Express **1**, 34 (2013).
[60]S. Habershon, B. J. Braams, and D. E. Manolopoulos, J. Chem. Phys. **127**(17), 174108 (2007).
[61]I. R. Craig and D. E. Manolopoulos, Chem. Phys. **322**(1–2), 236 (2006).
[62]J. Liu, B. J. Alder, and W. H. Miller, J. Chem. Phys. **135**(11), 114105 (2011).
[63]J. Liu and W. H. Miller, J. Chem. Phys. **127**(11), 114506 (2007).
[64]J. Liu and W. H. Miller, J. Chem. Phys. **129**(12), 124111 (2008).
[65]J. Liu and W. H. Miller, J. Chem. Phys. **128**(14), 144511 (2008).
[66]J. Liu, W. H. Miller, G. S. Fanourgakis, S. S. Xantheas, S. Imoto, and S. Saito, J. Chem. Phys. **135**(24), 244503 (2011).
[67]J. Liu, W. H. Miller, F. Paesani, W. Zhang, and D. A. Case, J. Chem. Phys. **131**(16), 164509 (2009).
[68]B. J. Ka and E. Geva, J. Phys. Chem. A **110**(31), 9555 (2006).
[69]B. J. Ka, Q. Shi, and E. Geva, J. Phys. Chem. A **109**(25), 5527 (2005).
[70]I. Navrotskaya and E. Geva, J. Phys. Chem. A **111**(3), 460 (2007).
[71]Q. Shi and E. Geva, J. Phys. Chem. A **107**, 9070 (2003).
[72]J. A. Poulsen, G. Nyman, and P. J. Rossky, J. Chem. Theory Comput. **2**(6), 1482 (2006).
[73]J. A. Poulsen, J. Scheers, G. Nyman, and P. J. Rossky, Phys. Rev. B **75**(22), 224505 (2007).
[74]J. A. Poulsen, G. Nyman, and P. J. Rossky, J. Phys. Chem. A **108**(41), 8743 (2004).
[75]J. A. Poulsen, G. Nyman, and P. J. Rossky, Proc. Natl. Acad. Sci. U.S.A. **102**(19), 6709 (2005).